Unsaturated Soils – Alonso & Gens (eds)
© 2011 Taylor & Francis Group, London, ISBN 978-0-415-60428-4

Laboratory determination of Soil-Water Characteristic Curves for cracked soil

M.M. Abbaszadeh, S. Houston, C. Zapata, W. Houston & B. Welfert
Arizona State University, Tempe, Arizona, USA

K. Walsh
San Diego State University, San Diego, California, USA

ABSTRACT: In general, unsaturated hydraulic conductivities are more difficult to estimate than are saturated, but as the soil transitions from intact to cracked, the difficulty in estimating the hydraulic conductivity and the water storage properties increases. One critical step in determination of unsaturated flow hydraulic properties lies in the evaluation of the Soil-Water Characteristic Curve (SWCC). In this paper, the authors' experience with a series of laboratory studies of direct measurements of cracked soil SWCCs is presented, including challenges associated with very low suction control. An oedometer-type SWCC apparatus, capable of suction and net normal stress control was used in these lab studies. This paper also addresses how the Air Entry Value (AEV) of the cracks can be calculated theoretically based on capillary theory, and the results are compared against AEVs determined from laboratory tests.

1 INTRODUCTION

The problem of estimating ground surface flux is one of great interdisciplinary interests, and the literature is replete with related articles from disciplines including soil science, geotechnical engineering, environmental ecology, hydrology, water resources, forestry, landscape architecture, geology, and environmental engineering. Surface flux is related to complex interrelationships between the soil and atmosphere, and soil anomalies such as cracks must be appropriately considered in any surface flux model. However, there is little data available for assessment of the effect of cracks on unsaturated flow properties, such as the Soil-Water Characteristic Curve (SWCC) and unsaturated hydraulic conductivity.

The properties and behavior of unsaturated cracked soil are potentially quite different from those of intact soil, and the absence of direct test data on cracked soil properties leads to uncertainty in the evaluation of surface flux conditions, particularly expansive soils. It is important to develop an improved understanding of cracked soil properties because seasonal cracking of soil results in poor estimates of runoff and infiltration due to the changing soil storage conditions (Arnold et al. 2005).

The primary objective of this paper is to present preliminary laboratory-scale SWCC test results on cracked soils. These data can be used, for example, to validate previously proposed bimodal models for fractured soils (Zhang & Fredlund 2004). These laboratory results provide much needed data for consideration of the effect of soils cracks on unsaturated soil property models, which has not been considered extensively.

2 BACKGROUND

Relationships for estimating unsaturated hydraulic conductivity based on the Soil-Water Characteristic Curve (SWCC) are commonly used, but have not been thoroughly evaluated for cracked soils. The measurement of the hydraulic conductivity for an unsaturated soil is extremely difficult, and the existence of cracks further complicates the measurement. For this reason, the SWCC has been used to predict the hydraulic conductivity of a cracked material (Peters & Klavetter 1988, Mallant et al. 1997, Köhne et al. 2002, Liu et al. 2004, Zhang & Fredlund 2004). Thus, one challenge for predicting the hydraulic conductivity of cracked soil is determining the SWCC. Once the SWCC is established for a cracked soil, it is likely that predictive models can be used to estimate the unsaturated hydraulic conductivity function. For example, Chertkov & Ravina (2000) studied the shrinking-swelling behavior of clay including a network of capillaries to represent cracks in the soil. The SWCC for the cracked soil was determined by using the total crack volume and the volume of water-filled cracks, and a generalization of the van Genuchten (1980)—Mualem (1976) model was used for estimating the unsaturated hydraulic

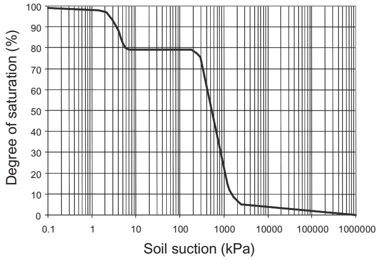

Figure 1. Typical Bimodal SWCC for Cracked Soil (Zhang & Fredlund 2004).

conductivity function. Liu and Bodvarsson (2001) studied the use of the van Genuchten (1980) and Brooks & Cory (1964) models for the hydraulic conductivity of a fractured rock. In this paper only the SWCC relationship is studied. On-going research by the authors will be directed towards validation of the use of existing SWCC-based predictive models for unsaturated hydraulic conductivity determination for cracked soils.

Zhang and Fredlund (2004) discuss that a fractured rock will produce a bimodal SWCC with a matrix phase and a fracture phase. The Soil-Water Characteristic Curve of the fractured rock was presented as the sum of the effects of the two phases, weighted according to their respective porosities. The combined matrix and fracture medium was treated as a continuum with the same suction applied to the combined material. A computed Soil-Water Characteristic Curve for the rock matrix, the fractures and the entire fractured rock mass is shown in Figure 1 (Zhang & Fredlund 2004). Taking a similar continuum approach to cracked soils, the Soil-Water Characteristic Curve takes on a bimodal character. Several mathematical models for the SWCC are available that allow for a bimodal SWCC (Durner 1994, Burger & Shackelford 2001, Gitirana & Fredlund 2004).

3 LABORATORY TESTING PROGRAM

Laboratory-scale tests were conducted to determine the SWCC for two artificially cracked compacted soil specimens. Only the drying curve of the SWCC is presented in this paper, although the study of SWCC hysteresis for cracked soils is the subject of on-going research by the authors. The suction range for these tests was 0.1–1300 kPa. An oedometer-type pressure plate device (Perez-Garcia, et al. 2008) was used to obtain the SWCC. A hanging manometer technique was used to apply very low matric suctions required to capture the bimodal nature of the SWCC. Theoretically, the existence of the cracks in the soil matrix will cause the soil to exhibit a bimodal behavior. The first hump in the bimodal SWCC is the AEV associated with the cracked phase, while the second hump is associated with the intact phase.

3.1 *Soil characteristics*

The soil used in this study was obtained from a site near San Diego, California. The basic index properties of the soil are presented in Table 1.

3.2 *Sample preparation*

Samples were initially compacted in three layers inside stainless steel rings having a height of 25 mm and diameter of 61 mm. Both samples were prepared with soil passing the No. 4 sieve and at 18% water content. The specimens were compacted to 90% of the standard Proctor maximum dry density. Following compaction, the cracks were created in the specimens using aluminum shims. These aluminum shims were varied in thickness to represent different crack widths. A total of 15 and 14 cracks were created for samples No. 1 and No. 2, respectively (Fig. 2). The depth of the cracks

Table 1. Soil characteristics.

Specific gravity		2.72
	% Sand	63
Particle size analysis	% Silt	30
	% Clay	7
Unified classification system		SC
Atterberg limits	LL	42
	PI	25
Standard proctor	Optimum water content	18%
	Max dry density (g/cm^3)	1.74
Expansion index (ASTM)		115

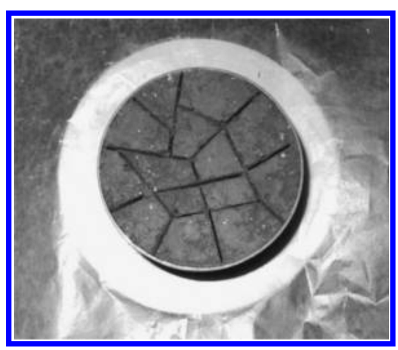

Figure 2. Artificially cracked sample No. 1 with 3.2% crack volume. (The crack volume for sample No. 2 was 4.4%).

ranged between 10 to 15 mm. The total volume of cracks was measured as a percentage of the overall specimen volume to be about 3 to 5%. A companion study was conducted with the same soil to evaluate the extent of cracks forming naturally due the drying and wetting cycles. From that study, it was concluded that the total volume of cracks was about 3–5% of the overall volume of the sample.

One challenge in dealing with cracks is the uncertainty associated with the contributions of various factors controlling the cracks' behavior. For example, the extent of crack healing during wetting is not entirely predictable. To capture the SWCC bimodal behavior, the cracks must be initially fully saturated, but should be wide enough so they will not heal completely upon saturation. Further, the cracks should be small enough to prevent desaturation by gravity drainage before any suction (air pressure) is applied using the pressure plate device. Based on preliminary observations, for the study soil, the cracks should be about 1.1–1.3 mm wide if a bi-model SWCC is to be observed in the laboratory. For this soil, cracks of 1.1–1.3 mm width were observed to shrink to 0.7–0.8 mm, after saturation.

Although soil crack patterns have been broadly documented (Wells et al. 2003, Scott et al. 1986, Konrad & Ayad 1997, Yesiller et al. 2000, Velde 1999, Young 2000, Vogel et al. 2005, Tang et al. 2008), there is not yet any widely dominant pattern of crack formation identified for field conditions. Despite some restrictions on creating the cracks artificially, however, we have tried to make the specimen crack patterns reasonably consistent with crack patterns found in nature.

3.3 *Test procedure, including aspects of testing at very low values of matric suction*

A hanging manometer technique was used to apply very low suctions. This method involves creating a negative pore water pressure (u_w), while keeping the pore air pressure (u_a) constant and equal to atmospheric pressure. This will result in matric suction being equal to the value of the negative pore water pressure because the matric suction is defined as $u_a - u_w$. As the water elevation inside the water tubes is positioned lower than the base elevation of the oedometer, the sample experiences suction equals to $-u_w$. For instance, to apply 0.1 kPa, one has to create the elevation difference equal to 1.0 cm between the water level in the tubes and the cell base (where the sample sits).

One of the major difficulties associated with setting a fixed low suction value is the continuous elevation change of the water that occurs inside the tube as the specimen seeks equilibration with the applied suction. Thus, the applied suction changes as the water elevation of the tube changes, and to keep the small applied suction constant, close monitoring is required on regular basis, becoming cumbersome in consideration of the lengthy test times required for equilibration, especially for highly plastic soils. Another point which makes tests at low suctions challenging is the fact that it is not possible to fully saturate the intact portion of the specimen because back-pressure saturation techniques are not easily employed in pressure plate testing. It was observed, at some very low suction stages of the SWCC test, that even after the specimen (likely the cracks in the specimen) released water at a prior, lower suction stages, the sample would tend to absorb water from the tube as the suction was increased (though still quite low). It is believed that this behavior is a result of the intact matrix part of the soil not having been fully saturated, even when the cracks were filled with water and extensive time for saturation of the specimen under submergence conditions had preceded the SWCC test. In other words, at early stages of the test, when the cracks are still full of water, the fractured phase of the soil dominates the behavior, while at later, higher suction stages, as the cracks dewatered, the intact soil matrix (not 100% saturated) governs the response.

4 THEORETICAL RELATIONSHIP BETWEEN WIDTH OF CRACK AND CAPILLARY RISE IN A CRACK

Should one idealize a soil crack as a capillary, there would always be a relationship between the width and depth of cracks which are capable of holding water inside of them. If the crack is too deep or too wide, the water cannot develop enough tension to overcome the self-weight of the water inside it, and as a result, the water will flow out of the crack, assuming the water pressure at the base of the crack is essentially zero.

First, the relationship will be derived between height of capillary rise, h_c, which will be assumed to be the crack depth, and the crack width, w_c. A continuous rectangular section throughout the crack depth is assumed, which is equivalent to saying the crack has a constant width from top to bottom, as shown in Figure 3. This assumption is of interest because cracks of this shape were generated in the laboratory.

Assuming the meniscus is fully developed and tangent to the side wall of the crack, the surface tension forces can be assumed to be vertical at the crack walls (Fig. 4) and equal to:

$$\text{Upward forces} = T_s \times 2\ \text{cm} \quad (1)$$

where, T_s = surface tension force per unit of length (73×10^{-5} N/cm); and 2 cm is the total

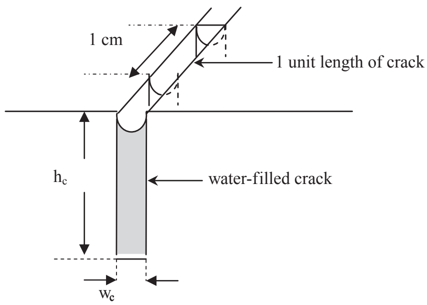

Figure 3. Schematic of constant width crack.

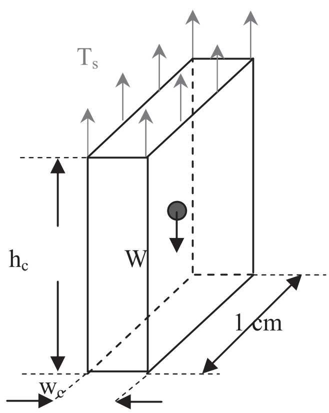

Figure 4. Free Body Diagram (FBD) of unit length water element in crack.

length over which surface tension acts, for a 1 cm segment.

The downward forces are equal to the weight of water and therefore, equal to the volume times the unit weight of water:

$$\text{Downward forces} = h_c \times w_c \times 1\text{ cm} \times \gamma_w \tag{2}$$

where, h_c = crack height; w_c = crack width; 1 cm = 1 unit length of crack; and γ_w = specific weight of water (9.807×10^{-3} N/cm^3).

For equilibrium in the vertical direction, upward forces are equal to the downward forces:

$$T_s \times 2\text{ cm} = h_c \times w_c \times 1\text{ cm} \times 9.807 \times 10^{-3} \tag{3}$$

Solving for h_c (with h_c and w_c in cm):

$$h_c = \frac{0.149}{w_c} \approx \frac{0.15}{w_c} \tag{4}$$

It should be noted that Equation 1 is based on several simplifying assumptions which are at variance with actual field conditions, but it is nevertheless potentially useful as a rough guide in estimating the AEV of the cracks.

Equation 4 was used to generate the results shown in Table 2, wherein the depth of crack ranges from 7 mm to 13 mm. This range in crack depth was chosen because, for this type of soil, naturally formed cracks, formed in laboratory condition, were about 10 mm deep, or slightly more. For each crack depth shown, it is assumed that the crack is full of water, the meniscus is fully developed and the surface tension at the top of the crack is just sufficient to balance the weight of water in the crack.

Because the suction is given by $u_a - u_w$ and the preceding derivation was made for the case of $u_a = 0$, the only component of suction is the water tension, u_w. Thus, the "corresponding suction" column in Table 2 can be thought of an equivalent AEV. At the suction shown, the dewatering is just commencing and air is starting to enter the crack.

At crack sizes smaller than those shown in Table 2, the capillary model would predict that dewatering due to gravity alone would not occur. However, if u_a were elevated to a value above zero, then u_a would generate an additional downward force which, together with the weight, could be made to overcome the surface tension forces. The derivation can be repeated along the same lines as before, but a new force due to u_a must be added to the free body diagram (Fig. 5).

Again, for a unit length of crack, Equation 1 remains unchanged, but Equation 2 can be rewritten as follows:

$$\text{Downward forces} = h_c \times w_c \times 1\text{ cm} \times \gamma_w + u_a (w_c \times 1\text{ cm}) \tag{5}$$

For equilibrium in the vertical direction, and solving for u_a (with h_c and w_c in cm) we get:

$$u_a = \frac{1.46 \times 10^{-3}}{w_c} - 9.807 \times 10^{-3} \times h_c \tag{6}$$

Table 2. Depth of crack and corresponding suction for which cracks of various widths will just start to dewater due to gravity alone.

Depth of crack, h_c		Corresponding suction = $h_c \times \gamma_w$	Width of crack that dewaters due to gravity alone	
cm	mm	kPa	cm	mm
0.7	7.0	0.069	0.21	2.1
1.0	10.0	0.098	0.15	1.5
1.3	13.0	0.127	0.11	1.1

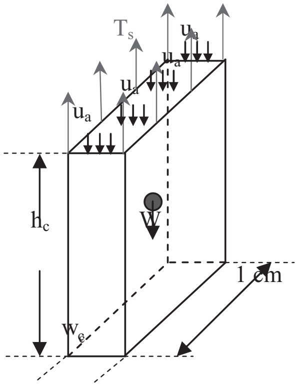

Figure 5. FBD including downward forces due to u_a.

Note that h_c controls u_w, which is given by $u_w = h_c \times \gamma_w$. Also, h_c controls the volume and weight of water in the crack. Due to these compensating effects, $u_a - u_w$ is insensitive to h_c, as shown in Tables 3a, 3b, and 3c. Figure 6 shows that u_a is also somewhat insensitive to h_c.

Now that different derivations were obtained for constant width crack, the same procedure can be used to derive new relationships for any shape of crack. For instance, in case of a V-shape crack, the analysis remains the same, except the volume of the unit length of water becomes one half of that obtained in the case shown above.

Table 3a. Relationship between h_c, w_c, and u_a for commencement of crack dewatering based on Equation 6, for $h_c = 0.7$ cm.

w_c		u_a		$u_w = h_c \times \gamma_w$	Suction $(u_a - u_w)$
cm	mm	N/cm^2	kPa	kPa	kPa
0.2	2.0	0.00044	0.0044	–0.0686	0.073
0.15	1.5	0.0029	0.029	–0.0686	0.098
0.1	1.0	0.0077	0.077	–0.0686	0.146
0.075	0.75	0.0126	0.126	–0.0686	0.195
0.05	0.50	0.022	0.22	–0.0686	0.289
0.01	0.10	0.139	1.39	–0.0686	1.459

Table 3b. Relationship between h_c, w_c, and u_a for commencement of crack dewatering based on Equation 6, for $h_c = 1.0$ cm.

w_c		u_a		$u_w = h_c \times \gamma_w$	Suction $(u_a - u_w)$
cm	mm	N/cm^2	kPa	kPa	kPa
0.15	1.5	0.0	0.0	–0.098	0.098
0.1	1.0	0.0048	0.048	–0.098	0.146
0.075	0.75	0.00967	0.0967	–0.098	0.195
0.05	0.50	0.0194	0.194	–0.098	0.292
0.01	0.10	0.1362	1.362	–0.098	1.46

Table 3c. Relationship between h_c, w_c, and u_a for commencement of crack dewatering based on Equation 6, for $h_c = 1.3$ cm.

w_c		u_a		$u_w = h_c \times \gamma_w$	Suction $(u_a - u_w)$
cm	mm	N/cm^2	kPa	kPa	kPa
0.1	1.0	0.0018	0.018	–0.128	0.146
0.075	0.75	0.0067	0.067	–0.128	0.195
0.05	0.50	0.0164	0.164	–0.128	0.292
0.01	0.10	0.133	1.33	–0.128	1.46

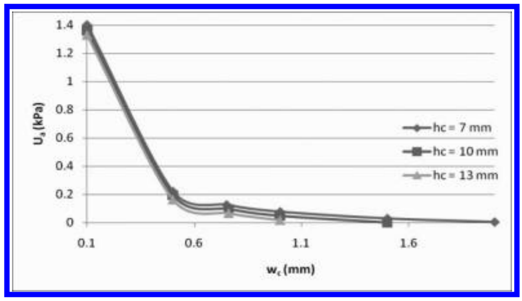

Figure 6. Relationship between h_c, w_c, and u_a for commencement of crack dewatering.

5 EXPERIMENTAL RESULTS

Quantification of a bimodal SWCC for cracked soil is difficult to accomplish for a variety of reasons, not the least of which is the difficulty in controlling the required extremely small suctions. It was possible to bracket the AEV on a test specimen as follows.

An SWCC test specimen was prepared with cracks of an initial width, w_c, of about 1 mm and a depth, h_c, of about 10 mm. After wetting to essentially saturation a slight closing of the cracks was observed, to a width of about 0.75 mm. A value of u_a of about 0.07 kPa was applied and the specimen was subsequently observed after time for equilibrium. A few of the cracks showed signs of starting to dewater. The test chamber was resealed and a new u_a value of 0.1 to 0.2 kPa, say 0.15 kPa, was applied and allowed to equilibrate. Subsequent examination of the cracks showed that they were more or less completely dewatered. Thus, the u_a causing initiation of dewatering was somewhere between 0.07 kPa and 0.15 kPa, experimentally, and perhaps closer to 0.07 kPa.

Of course, soil suction is given by $u_a - u_w$, but it is common practice in both SWCC testing and triaxial shear testing, when using the axis translation technique, to neglect u_w and simply equate suction to the imposed u_a. However, for the case at hand, the u_a values are so small that u_w values are not necessarily negligible. Accordingly, $u_a - u_w$ was calculated for Table 3 using non-zero values in general for both u_a and $-u_w$.

For the purpose of comparing the experimental results with the theoretical results, it is most convenient to simply assume the u_w values in the laboratory test specimen were the same as for the matching boundary conditions in the capillary model (Table 3). Then the comparison amounts to simply comparing the u_a applied in the lab to the value of u_a computed and entered in Table 3.

If the w_c is 0.75 mm and values from Table 3b are used, for which $h_c = 1.0$ cm, a value of $u_a \approx 0.1$ kPa is obtained. This value compares very well with the measured range of 0.07 to 0.15 kPa. For the meager amount of experimental data available to date, the capillary model compares very well with experimental data.

Interestingly, the SWCCs for intact and cracked samples were found reasonably close after crack desaturation, as can be seen in Figure 7 where the curves are tending to merge at higher suctions. According to the tests conducted for cracked samples, bimodal behavior of the cracked soil is observed. The major difference between the cracked and intact curves is the initial volumetric water content, which should be expected, since the 3 to 4% crack volume significantly impacted the overall void ratio. These crack voids were almost completely saturated during the wetting process. Consequently, the volumetric water content would be higher for cracked sample compared to an intact sample. As the suction increases from zero to 0.1 kPa, for these particular sizes of the cracks, nearly all of the cracks dewater, and the first break in the curve corresponds to the AEV of the cracks. The second break in the curve occurs somewhat above 10 kPa and is believed to represent the AEV of the intact matrix.

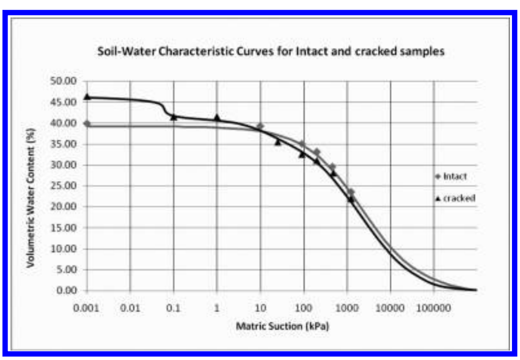

Figure 7. Comparison between cracked and intact SWCC for the same samples.

6 CONCLUSION

More comparisons would be needed before elevating the capillary model to a predictive model that should be used in lieu of measurements. But the comparison above strengthens the initial assumption that the capillary model can be used to obtain at least a rough estimate of AEV for cracks.

Experimental results to date show that the SWCC for a cracked soil can be represented by a bimodal curve. However, the AEV of the cracks is very low, even for the relatively small width cracks considered in the laboratory study. Dewatering of larger field cracks would be expected to occur at extremely low suction values, and perhaps to dewater under gravity alone.

ACKNOWLEDGEMENT

This study was supported by the National Science Foundation (NSF) under grant number CMMI-0825089. The opinions, conclusions, and interpretations expressed in this paper are those of the authors, and not necessarily of NSF.

REFERENCES

Arnold, J.G., Potter, K.N., King, K.W. & Allen, P.M. 2005. Estimation of soil cracking and the effect on surface runoff in a Texas Blackland Prairie Watershed. Hydrol. Process 19(3): 589–603.

Brooks, R.H., & Corey, A.T. 1964. Hydraulic properties of porous media. Colorado State University Hydrology Paper, Fort Collins Nr. 3, Vol. 27, March.

Burger, C.A. & Shackelford, C.D. 2001. Soil-Water Characteristic Curves and dual porosity of sand-diatomaceous earth mixtures. J. of Geotechnical and Geoenvironmental Engineering, ASCE 127(9): 790–800.

Chertkov, V.Y. & I. Ravina. 2000. Shrinking-swelling phenomenon of clay soils attributed to capillary-crack network. Theoretical and Applied Fracture Mechanics 34: 61–71.

Durner, W. 1994. Hydraulic conductivity estimation for soil with heterogeneous pore structure. Water Resources Research 30(2): 211–223.

Gitirana, Jr. G. & Fredlund, D.G. 2004. Equations for the soil-water characteristic curve based on meaningful and mathematically independent parameters. ASCE J. of Geotechnical and Environmental Engineering 130(2): 209–212.

Konrad J.M. & Ayad, R. 1997. Desiccation of a sensitive clay: field experimental observations. Can. Geotech. J. 34: 929–942.

Köhne, J.M., Köhne, S. & Gerke H.H. 2002. Estimating the hydraulic functions of dual-permeability models from bulk soil data. Water Resources Research 38(7): 1121–1132.

Liu, H.H. & Bodvarsson, G.S. 2001. Constitutive relations for unsaturated flow in a fracture network. J. of Hydrology 252: 16–25.

Liu. H.H., Bodvarsson, G.S. & Finsterle. S. 2004. A note on unsaturated flow in two-dimensional fracture networks. Technical Note. Earth Sciences Division. Lawrence Berkeley National Laboratory. Uni. of Calif., Berkeley.

Mallant, D., Tseng, P.H., Torde, N., Timmerman, A. & Feyen, J. 1997. Evaluation of multimodal hydraulic function in characterizing a heterogeneous field soil. J. of Hydrology 195: 172–199.

Mualem, Y. 1976. A new model for predicting the hydraulic conductivity of unsaturated porous media. Water Resources Research 12: 593–622.

Perez-Garcia, N., Houston, S., Houston, W., Padilla, J.M. (2008). An Odometer-Type Pressure Plate SWCC Apparatus, ASTM Geotech. Testing J., March.

Peters, R.R. & Klavetter, E.A. 1988. A continuum model for water movement in unsaturated fractured rock mass. Water resources research 24(3): 416–430.

Scott, G.J., Webster R. and Nortcliff S. An analysis of crack pattern in clay soil: its density and orientation, J. Soil Sci. 37 (1986), pp. 653–668

Tang, C., Shi, B., Liu, C., Zhao, L., & Wang, B. 2008. Influencing factors of geometrical structure of surface shrinkage cracks in clayey soils. Engineering Geology 101: 204–217.

Van Genuchten, M. Th. 1980. A closed form equation for predicting the hydraulic conductivity of unsaturated soils. Soil Sci. Soc. Am. J. 44: 892–898.

Velde, B. 1999. Structure of surface cracks in soil and muds. Geoderma 93: 101–124.

Vogel, H.J., Hoffmann, H. & Roth K. 2005. Studies of crack dynamics in clay soil I. Experimental methods, results, and morphological quantification. Geoderma 125: 213–223.

Wells, R.R., DiCarlo, D.A., Steenhuis, T.S., Parlange, J.Y., Romkens, M.J.M. & Prasad, S.N. 2003. Infiltration and surface geometry features of a swelling soil following successive simulated rainstorms. Soil Science Society of America Journal 67(5): 1344–1351.

Yesiller, N., Miller, C.J., Inci G. & Yaldo, K. 2000. Desiccation and cracking behavior of three compacted landfill liner soils. Engineering Geology 57: 105–121.

Young, I.M. 2000. An empirical stochastic model for the geometry of two-dimensional crack growth in soil (with Discussion). Geoderma 96: 263–289.

Zhang, L. & Fredlund, D.G. 2004. Characteristics of water characteristic curves for unsaturated fractured rocks. The Second Asian Conference on Unsaturated Soils, Unsat-Asia, Osaka, Japan: 425–428.